

# Chip-based frequency combs with sub-100 GHz repetition rates

Adrea R. Johnson,<sup>1,\*</sup> Yoshitomo Okawachi,<sup>1</sup> Jacob S. Levy,<sup>2</sup> Jaime Cardenas,<sup>2</sup>  
Kasturi Saha,<sup>1</sup> Michal Lipson,<sup>2,3</sup> and Alexander L. Gaeta<sup>1,3</sup>

<sup>1</sup>*School of Applied and Engineering Physics, Cornell University, Ithaca, New York 14853, USA*

<sup>2</sup>*School of Electrical and Computer Engineering, Cornell University, Ithaca, New York 14853, USA*

<sup>3</sup>*Kavli Institute at Cornell for Nanoscale Science, Cornell University, Ithaca, New York 14853, USA*

\*Corresponding author: arj46@cornell.edu

Received December 1, 2011; revised January 20, 2012; accepted January 20, 2012;

posted January 23, 2012 (Doc. ID 159146); published February 24, 2012

By fabricating high- $Q$  silicon-nitride spiral resonators, we demonstrate frequency combs spanning over 200 nm with free spectral ranges (FSRs) of 80, 40, and 20 GHz using cascaded four-wave mixing. We characterize the RF beat note for the 20 GHz FSR comb, and the measured linewidth of 3.6 MHz is consistent with thermal fluctuations in the resonator due to amplitude noise of the pump source. These combs represent an important advance towards developing a complementary metal-oxide-semiconductor (CMOS)-based system capable of linking the optical and electronic regimes. © 2012 Optical Society of America

OCIS codes: 140.3948, 190.4380, 190.4390.

Frequency combs have broad applications in spectroscopy, astronomy, remote sensing, frequency metrology, high-speed coherent communications, arbitrary waveform synthesis, and optical clocks [1–3]. Frequency combs with a free spectral range (FSR) less than 100 GHz provide a direct link between optical and electrical signals, since these optical signal frequencies are detectable using fast photodiodes and could be used to produce highly stable microwave signals [4]. Recently, there has been significant research in the generation of frequency combs utilizing parametric oscillation in high- $Q$  microcavities [5]. The generation of such combs occurs via four-wave mixing (FWM) parametric oscillation that cascades to produce new frequency components at modes of the resonator. Frequency combs have been demonstrated in platforms including silica microtoroids [6,7],  $\text{CaF}_2$  resonators [8,9],  $\text{MgF}_2$  resonators [10,11], silica microspheres [12], high-index silica-glass microrings [13], and silicon-nitride microrings [14–18], and there have been initial theoretical studies to understand comb generation in such systems [19].

Silicon-nitride microrings are particularly attractive for chip-based comb generation, since the resonator and the coupling waveguide are monolithically integrated, which provides an on-chip frequency comb source that is robust and environmentally isolated. The fabrication process is complementary metal-oxide-semiconductor (CMOS) compatible and, unlike the whispering gallery resonator geometries, offers the flexibility to separately control the dispersion of the waveguide and the comb line spacing. The ability to tailor the group-velocity dispersion (GVD) over a wide bandwidth enables phase-matching conditions necessary for efficient and broadband FWM-based parametric oscillation, and the capability to pump and generate combs from the near visible to midinfrared regimes [16]. Many previous demonstrations [14–18] of combs generated in microrings have yielded relatively large comb spacings, which cannot be readily used to link optical and microwave regimes. Recently, lower repetition rate FSRs have been demonstrated in fused-quartz (36 GHz) [20],  $\text{MgF}_2$  (35 GHz) [21],  $\text{Si}_3\text{N}_4$  (76 GHz) [21],

and  $\text{SiO}_2$  disk resonators (22.9 GHz) [22]. Our novel design of silicon-nitride spiral resonators comprises the first integrated platform for achieving broad spectrum, low repetition rate, and low phase noise frequency combs.

In this Letter, we demonstrate, for the first time, frequency comb generation in silicon-nitride resonators with repetition rates as low as 20 GHz. Pumping with a single frequency laser at 1560 nm, we are able to generate frequency combs that span over 200 nm with FSRs of 80, 40, and 20 GHz. In addition, we characterize the RF beat note of the 20 GHz FSR comb and find that the observed linewidth is consistent with thermal fluctuations in the resonator. Our design shows promise as a stable, integrated frequency comb source at RF repetition rates that can be designed to operate at wavelengths in the near visible to midinfrared.

The GVD is engineered by varying the cross section of the spiral resonator waveguide. We use a finite-element mode solver to ascertain the cross section that yields large anomalous GVD over the specified wavelength range. In turn, the FSR is tailored by adjusting the path length of the resonator. Our design to produce combs with lower repetition rates is based on silicon-nitride spiral resonators in which each resonator is designed to fit on a single field of the electron beam lithography tool in order to avoid stitching errors during fabrication, which can lead to higher losses. Fabrication of the spiral resonators starts with a silicon dioxide undercladding layer grown on a silicon wafer [14]. A silicon-nitride layer is then deposited using low-pressure chemical vapor deposition, and the resonator and bus waveguide are patterned with an electron beam resist and etched with a reactive ion etch. Lastly, a layer of silicon dioxide is deposited as the top cladding.

Simulations of the group index allow us to calculate the path length required for each FSR. To achieve FSRs of 80, 40, and 20 GHz, the path length of the resonators must be increased to 1.8, 3.6, and 7.2 mm, respectively. In order to maintain low losses, it is essential that the resonator be fabricated within a single  $e$ -beam field to avoid stitching errors at the boundaries. These increased path

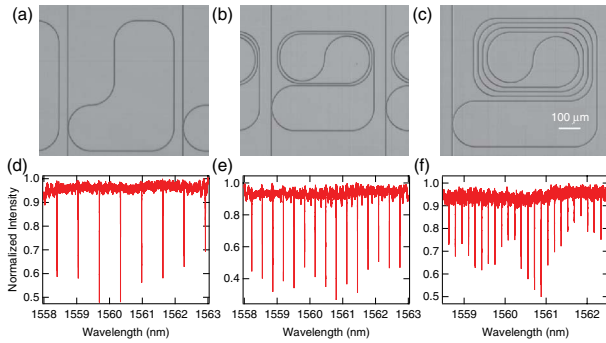


Fig. 1. (Color online) Micrographs of the (a) 80-, (b) 40-, and (c) 20 GHz FSR resonators and the corresponding transmission spectra for (d), (e), and (f), respectively.

lengths will no longer fit on a single  $e$ -beam field using the simple ring geometry employed in all previously demonstrated parametric-combs, and thus we fabricate a specific spiral geometry for each resonator (Fig. 1). We employ a constant semicircular coupling region in all cases to enable critical coupling between the bus waveguide and the resonator independent of path length. Bends in the resonators have radii greater than  $100\ \mu\text{m}$  to ensure that the dispersion introduced by the bends is negligible as compared to the dispersion in the straight sections, which is critical for proper operation of the frequency comb.

To characterize the quality factor of the spiral resonators, we perform transmission measurements in which a lensed fiber injects quasi-TE polarized light from a tunable cw laser into the bus waveguide and an objective collects the output light. A power meter monitors the output power as the laser scans over a 4 nm wavelength range from 1558.5 to 1562.5 nm. Figures 1(d)–1(f) show the transmission measurements, respectively, for the 80-, 40-, and 20 GHz FSR resonators. The data are postprocessed to remove weak Fabry–Perot fringes that occur due to the detector. The loaded quality factor calculated from this transmission spectrum for the 20 GHz FSR resonator is  $8 \times 10^5$ , and the 40- and 80 GHz FSR resonators yield quality factors of similar magnitude.

For frequency comb generation, the pump source consists of a tunable cw laser at 1560 nm amplified by an erbium-doped fiber amplifier (EDFA). A combination of a fiber polarization controller and polarizer allows adjustment of the input polarization to quasi-TE. The frequency comb spectrum is monitored on an optical spectrum analyzer. We use a waveguide cross section of 1650 nm by 725 nm to produce anomalous GVD at the pump wavelength [17]. Input coupling loss to the bus waveguide is 5 dB. As the pump laser is tuned to a cavity resonance, optical parametric oscillation and the generation of a signal and idler pair occur when the roundtrip parametric gain exceeds the cavity loss. Increasing the power beyond the threshold for parametric oscillation results in cascaded FWM and the generation of multiple wavelengths. The comb is filled through higher-order degenerate and nondegenerate FWM processes.

The experimentally measured spectra for the 80, 40, and 20 GHz microresonators are shown in Fig. 2. The 40- and 80 GHz combs require 2.1 W, and the 20 GHz requires 2.2 W to fill the entire comb spans, which are

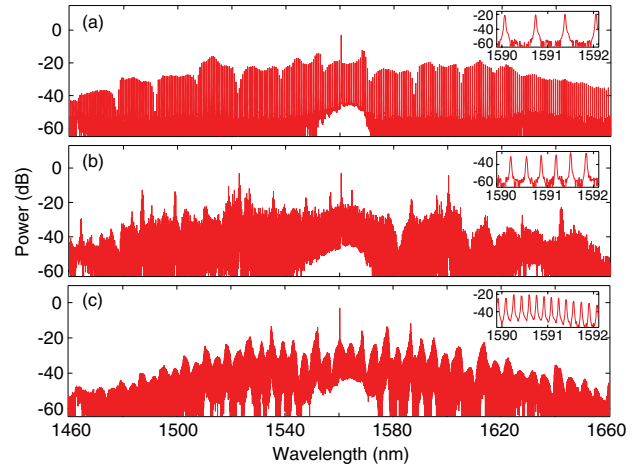


Fig. 2. (Color online) Frequency spectra generated from microresonators with FSRs of (a) 80 GHz, (b) 40 GHz, and (c) 20 GHz. A 2 nm section of each comb is inset in each figure to illustrate the spacing of the comb lines.

300 nm for the former two and 200 nm for the latter. Similar to [17], we observe that the amplitude noise of the combs, characterized with an RF spectrum analyzer, shows a reduction in the noise level during comb generation, which we believe is due to the system reaching a phase-locked state. The modulations in the 20 GHz comb spectrum result from the fact that, while it is sufficient for reaching the low-noise state, the coupled power is insufficient for equalization of the comb lines. Each inset in Fig. 2 shows a high-resolution view of the respective comb in the low-noise state.

We characterize in more detail the spacing of the 20 GHz comb by measuring the RF beat note. A 1 nm section of the comb spectrum is filtered at 1540 nm and amplified with an EDFA. The output is sent to a fast photodiode detector and measured with an RF spectrum analyzer. Figure 3(a) shows the detected RF beat note (red line) and background noise measurement (blue line), which shows the detector response. The RF beat note has a frequency of 19.83 GHz with a full width at half maximum (FWHM) of 3.6 MHz, which is significantly narrower than previous observations [21]. Additionally,

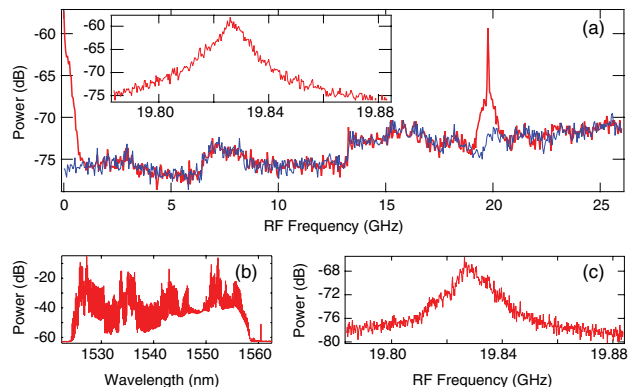


Fig. 3. (Color online) (a) Measured RF frequency for the 20 GHz comb with a peak at 19.83 GHz (red trace) and background measurement (blue trace). Inset shows a magnified view of the peak. (b) Filtered 30 nm segment of the 20 GHz comb. (c) RF frequency spectrum for 30 nm segment.

we perform a beat note measurement with a 30 nm section of the comb [Fig. 3(b)]. The linewidth of the beat note, shown in Fig. 3(c), remains unchanged with the 30× increase in the filtered spectral width, thereby confirming that our measured linewidth is not due to variations in comb spacing. We have observed previously that pump power fluctuations lead to thermal changes in the resonator that shift both the resonance and FSR [17]. We believe that our measured linewidth is limited primarily by the amplitude noise from the EDFA and the laser. We estimate a frequency shift of approximately 100 kHz/mW with respect to coupled power in the bus waveguide.

In conclusion, we demonstrate the generation of frequency combs spanning over 200 nm with FSRs of 20, 40, and 80 GHz using silicon-nitride spiral ring resonators. We detect the 20 GHz comb spacing with a fast photodiode, illustrating that such chip-based combs are capable of bridging the gap between optical and microwave frequencies, and we find that the measured linewidth of the comb lines is consistent with thermal variations of the index of the microresonator. Combs with FSRs in this microwave regime will allow for advancements in astronomy, metrology, high-speed coherent communications, optical clocks, and high-precision microwave sources. This platform yields a compact, stable, and integrated comb source that is CMOS compatible, which could allow for future integration with other photonic and electronic components.

We acknowledge support from DARPA and the Center for Nanoscale Systems, supported by the NSF and the New York State Foundation for Science, Technology, and Innovation. This work was performed in part at the Cornell NanoScale Facility, a member of the National Nanotechnology Infrastructure Network, which is supported by the NSF (grant ECS-0335765). A. R. J., Y. O., and J. S. L. contributed equally to this work.

## References

1. T. Udem, R. Holzwarth, and T. W. Hänsch, *Nature* **416**, 233 (2002).
2. Z. Jiang, D. E. Leaird, and A. M. Weiner, *Opt. Express* **13**, 10431 (2005).
3. T. Steinmetz, T. Wilken, C. Araujo-Hauck, R. Holzwarth, T. Hänsch, L. Pasquini, A. Manescau, S. D'Odorico, M. T. Murphy, T. Kentischer, W. Schmidt, and T. Udem, *Science* **321**, 1335 (2008).
4. A. Bartels, S. A. Diddams, C. W. Oates, G. Wilpers, J. C. Bergquist, W. H. Oskay, and L. Hollberg, *Opt. Lett.* **30**, 667 (2005).
5. T. J. Kippenberg, R. Holzwarth, and S. A. Diddams, *Science* **332**, 555 (2011).
6. P. Del'Haye, A. Schliesser, O. Arcizet, T. Wilken, R. Holzwarth, and T. J. Kippenberg, *Nature* **450**, 1214 (2007).
7. P. Del'Haye, T. Herr, E. Gavartin, R. Holzwarth, and T. J. Kippenberg, *Phys. Rev. Lett.* **107**, 063901 (2011).
8. I. S. Grudin, N. Yu, and L. Maleki, *Opt. Lett.* **34**, 878 (2009).
9. A. A. Savchenkov, A. B. Matsko, V. S. Ilchenko, I. Solomatine, D. Seidel, and L. Maleki, *Phys. Rev. Lett.* **101**, 093902 (2008).
10. C. Y. Wang, T. Herr, P. Del'Haye, A. Schliesser, J. Hofer, R. Holzwarth, T. W. Hänsch, N. Picqué, and T. J. Kippenberg, arXiv:1109.2716 (2011).
11. W. Liang, A. A. Savchenkov, A. B. Matsko, V. S. Ilchenko, D. Seidel, and L. Maleki, *Opt. Lett.* **36**, 2290 (2011).
12. I. H. Agha, Y. Okawachi, and A. L. Gaeta, *Opt. Express* **17**, 16209 (2009).
13. L. Razzari, D. Duchesne, M. Ferrera, R. Morandotti, S. Chu, B. E. Little, and D. J. Moss, *Nat. Photon.* **4**, 41 (2010).
14. J. S. Levy, A. Gondarenko, M. A. Foster, A. C. Turner-Foster, A. L. Gaeta, and M. Lipson, *Nat. Photon.* **4**, 37 (2010).
15. M. A. Foster, J. S. Levy, O. Kuzucu, K. Saha, M. Lipson, and A. L. Gaeta, *Opt. Express* **19**, 14233 (2011).
16. Y. Okawachi, K. Saha, J. S. Levy, M. A. Foster, M. Lipson, and A. L. Gaeta, in *CLEO:2011—Laser Applications to Photonic Applications*, Technical Digest (CD) (Optical Society of America, 2011), paper CFK2.
17. Y. Okawachi, K. Saha, J. S. Levy, Y. H. Wen, M. Lipson, and A. L. Gaeta, *Opt. Lett.* **36**, 3398 (2011).
18. F. Ferdous, H. Miao, D. E. Leaird, K. Srinivasan, J. Wang, L. Chen, L. T. Varghese, and A. M. Weiner, *Nat. Photon.* **5**, 770 (2011).
19. Y. K. Chembo and N. Yu, *Phys. Rev. A* **82**, 033801 (2010).
20. S. Papp and S. Diddams, *Phys. Rev. A* **84**, 053833 (2011).
21. T. Herr, J. Riemensberger, C. Wang, K. Hartinger, E. Gavartin, R. Holzwarth, M. L. Gorodetsky, and T. J. Kippenberg, arXiv:1111.3071 (2011).
22. J. Li, H. Lee, T. Chen, and K. Vahala, in *FiO:2011—Laser Science*, Technical Digest (CD) (Optical Society of America, 2011), paper FWB2.